

The 1s x-ray absorption pre-edge structures in transition metal oxides

This article has been downloaded from IOPscience. Please scroll down to see the full text article.

2009 J. Phys.: Condens. Matter 21 104207

(<http://iopscience.iop.org/0953-8984/21/10/104207>)

View [the table of contents for this issue](#), or go to the [journal homepage](#) for more

Download details:

IP Address: 129.252.86.83

The article was downloaded on 29/05/2010 at 18:31

Please note that [terms and conditions apply](#).

The 1s x-ray absorption pre-edge structures in transition metal oxides

Frank de Groot¹, György Vankó² and Pieter Glatzel³

¹ Inorganic Chemistry and Catalysis, Utrecht University, Sorbonnelaan 16, 3584 CA Utrecht, Netherlands

² KFKI Research Institute for Particle and Nuclear Physics, PO Box 49, H-1525 Budapest, Hungary

³ European Synchrotron Radiation Facility, BP 220, 38043 Grenoble Cédex, France

E-mail: f.m.f.degroot@uu.nl

Received 2 October 2008, in final form 18 November 2008

Published 10 February 2009

Online at stacks.iop.org/JPhysCM/21/104207

Abstract

We develop a general procedure to analyse the pre-edges in 1s x-ray absorption near edge structure (XANES) of transition metal oxides and coordination complexes. Transition metal coordination complexes can be described from a local model with one metal ion. The 1s 3d quadrupole transitions are calculated with the charge-transfer multiplet program. Tetrahedral coordination complexes have more intense pre-edge structures due to the local mixing of 3d and 4p states, implying a combination of 1s 3d quadrupole and 1s 4p dipole transitions. Divalent transition metal oxides can be described similar to coordination complexes, but for trivalent and tetravalent oxides, additional structures are visible in the pre-edge region due to non-local dipole transitions. The 1s 4p dipole transitions have large cross section at the 3d-band region due to the strong metal–metal interactions, which are oxygen mediated. This yields large intensity in the 3d-band region but at a different energy than the local 1s 3d quadrupole transitions because of smaller core-hole effects due to the delocalization of the excited electron.

(Some figures in this article are in colour only in the electronic version)

1. Introduction

The 1s XANES pre-edge structures of transition metal oxides are reviewed. The general understanding is that the 1s core levels can be explained with the single electron excitation model, while the 2p XAS spectra need a charge-transfer multiplet analysis, in particular for 3d transition metal systems. Using the single electron excitation model, the 1s XANES spectra are divided into the main edge due to transitions from the 1s core state to the 4p conduction band. Below the main edge are, in some cases, minor peaks visible that are denoted as pre-edge structure. These pre-edge structures are assigned as quadrupole transitions from the 1s core state to the empty 3d states. In case the inversion symmetry of the transition metal is broken, the pre-edge gains additional intensity due to the local 3d 4p wavefunction mixing, effectively allowing dipole transitions to the 4p character of the 3d-band.

The dipole selection rules state that the 1s core electron is excited to the lowest possible states with p character. In a first-row transition metal oxide the lowest empty metal p state is the 4p-band that is formed from the anti-bonding combinations of

the metal 4p states with the oxygen 2p states. We postpone a detailed description of the pre-edge structures and assume for the moment that the pre-edge relates to the quadrupole transitions to the empty 3d states.

The theoretical simulation of the transition metal K edge spectra can be performed with any single particle excitation model that describes the empty density of states [1]. One can use band structure codes such as PARATEC [2, 3], WIEN2K [4], CASTEP [5] or real space multiple scattering codes such as FDMNES [6], FEFF [7], CONTINUUM [8] and MXAN [9]. All these codes can reproduce in many cases the metal K edge XANES accurately, where it is noted that because of the 1s lifetime broadening of more than 1 eV, these calculations need to be correct only within this resolution.

The first detailed 1s XANES experiments were performed in the early eighties. The interpretation of the spectra was based on calculations either by multiple scattering [10] or band structure methods [11]. Grunes noted that one should include the response to the core hole as well as the excited-electron core-hole interaction, but the good agreement between single particle excitation calculations and experiment

indicated that such effects could be neglected, at least with the experimental resolution that was available [11]. Detailed band structure calculations of the transition metal K edges have been performed by Muller *et al* [12] and early multiple scattering calculations of the transition metal oxide K edges were carried out by Norman *et al* [13]. Important additions in these interpretations included the use of extended basis sets and the inclusion of the core-hole potential [14].

More recent band structure and multiple scattering calculations use final-state calculations including the core-hole potential and the K edge spectrum can be calculated over the whole XANES region. For example, Wu *et al* analyse the 1s XANES of a series of transition metal oxides (MnO, FeO, CoO, NiO) and they found a good agreement between their multiple scattering calculations and the experimental spectra [8]. The pre-edge is calculated as a quadrupole transition. In the experimental K edge spectrum, the pre-edge is essentially a single peak, which is also found in the calculations with the broadening as applied. Also with multiple scattering calculations using FEFF [7], good agreement between the metal K edge and the calculated spectrum is found, where it can be shown that the spectral shape essentially reproduces the metal p-projected density of states, for example in the case of CaO [15]. In these calculations it is important to include the core-hole potential in order to reproduce the details of the spectral shape. Recent band structure calculations are able to reproduce the metal K edge XANES spectra in great detail. The PARATEC calculations from Cabaret *et al* [16] reproduce the TiO₂ K edge including its angular dependence. Juhin *et al* show the one-to-one correspondence between the empty density of states and the Cr K edge XANES of Cr impurities in MgAl₂O₄ [17].

These results show that the 1s XANES can be accurately described with single electron excitation calculations based on multiple scattering or band structure calculations. That such good agreement is found is actually rather surprising, because of the neglect of charge-transfer effects: the 1s core hole will pull down the 3d states, yielding, in principle, a combination of a well screened peak and a poorly screened peak, similar to the case of core level photoemission spectra. This phenomenon was originally described by Bair and Goddard [18] and observed by Tolentino *et al* [19] in case of La₂CuO₄. Recently, this model was also used by Collart *et al* [20], who selectively excite the 1s¹ 3d⁹ \underline{L} 4p¹ peak and the 1s¹ 3d⁸ 4p¹ peak in La₂NiO₄ to measure the corresponding RXES spectra. As has been discussed, the majority of K edge XANES simulations omit these charge-transfer effects and still find very good agreement.

Qualitative analysis of transition metal K edges has been important for the practical application of the technique. These qualitative analysis methods are based on the density of states interpretation and use characteristic features of the pre-edge and edge region to determine trends within related compounds. An initial qualitative relation between the 1s XANES spectra with site geometry and valence was provided by Kau *et al* [21] for copper compounds. In an extensive XANES study on iron minerals, Waychunas found a correlation between the bond angle variance, a measure for the site distortion,

and the normalized pre-edge intensity [22]. Wilke and co-workers extended this relation and they determined that there is a correlation between pre-edge intensity with the local site symmetry [23]. In addition they found a correlation between the energy of the pre-edge barycentre correlates with the valence. These rules have been applied to Fe and Mn impurities in zeolite systems [24, 25]. Wong *et al* [26] found that the pre-edge and the edge shift with different energy scales. This provides an internal measure for the valence determination [27]. These empirical correlations show that also without a detailed theoretical foundation, pre-edge and edge structures can be used to derive useful information. The amount of information that can be extracted from an edge analysis can be considerably increased, though, with the development of more detailed theoretical analyses.

In this paper we will refine the interpretation of the 1s XANES spectra of transition metal systems. We will show that, in addition to the density of state based structures described above, additional peaks are present depending on the valence, local symmetry and the metal–metal distances.

2. HERFD-XANES spectra

An important improvement in the determination of spectral details for the K pre-edge structure is the development of high-energy resolution fluorescence detected (HERFD) x-ray absorption. XANES spectra can be measured with a fluorescence detector with an energy resolution that is similar to the core hole lifetime broadening. In the energy range of the transition metal K edges these detectors are based on perfect crystal Bragg optics. The common Rowland geometry uses spherically bent crystals with a suitable Bragg reflection at a specific x-ray emission energy and the x-rays are focussed on a photon counter. These detectors and the experiments that can be performed with them are discussed, for example in the review paper by Glatzel and Bergmann [28] and also in the book Core Level Spectroscopy of Solids [29]. Hamalainen *et al* [30] showed that in such measurements the life time broadening of the 1s core hole no longer appears in the spectra.

As an example, the cobalt K edge x-ray absorption spectra of CoO is given in figure 1. The normal K edge XANES spectrum (dashed) is given in comparison with the HERFD-XANES (red, solid). The pre-edge is visible between 7706 and 7710 eV. The edge start at approximately 7715 eV. The large amount of additionally resolved structures in the 1s HERFD-XANES spectrum of CoO can be used as an example to show how accurate the band structure and multiple scattering calculations are in reproducing these features.

3. The 1s pre-edge structures

3.1. The pre-edge structures in coordination complexes

For the interpretation of the XANES spectra, coordination complexes are considered as isolated metal ions, surrounded by ligands. The general model to interpret pre-edges is to consider them as quadrupole transitions into the empty 3d

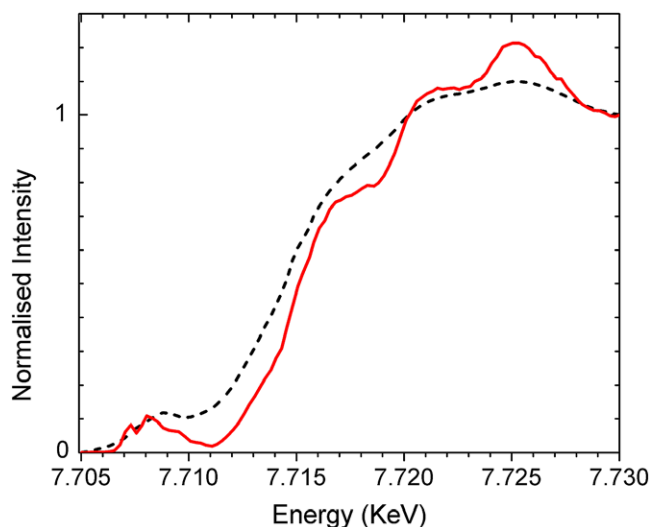


Figure 1. The cobalt 1s XANES spectrum of CoO. Shown are the normal XAS spectrum (dashed), as measured with a solid state fluorescence detector and the HERFD-XANES spectrum (red, solid).

states. Quadrupole transitions have intrinsic transition strength of approximately 0.1% of the dipole transitions, but because of the high density of states for the 3d-band they are visible as small peaks with $\sim 1\text{--}3\%$ intensity in most, octahedral, transition metal systems. If inversion symmetry is broken, for example in tetrahedral coordination complexes, the metal 3d and 4p states mix and there are direct dipole transitions into the 4p character of the 3d-band.

Octahedral coordination complexes only have quadrupole transitions and these transitions can be simulated from $3d^N$ to $1s^1 3d^{N+1}$ multiplet calculations. Figure 2 shows these $3d^N \rightarrow 1s^1 3d^{N+1}$ calculations, for $N = 0\text{--}9$. The final state contains a 1s core hole, but the 1s 3d interaction has no effect on the energy splittings of the pre-edge structures. In fact, the complete structure is determined by the $3d^{N+1}$ multiplet positions and their coupling to the ground state. If one neglects the small 3d spin-orbit coupling this approach has been used by Westre *et al* [31] to explain the pre-edge structures in iron coordination complexes.

It can also be shown that charge-transfer effects have little effect on the 1s 3d quadrupole pre-edge spectral shapes. Figure 3 shows the difference between an ionic and a charge-transfer calculation. With the parameters used a significant charge-transfer state was visible in the iron L edge, but the K edge shows almost no charge-transfer structures. These crystal field multiplet calculations reproduce the pre-edge structures of a series of iron coordination complexes [31, 32] and manganese coordination complexes [33]. In fact, also many bulk transition metal oxide systems can be reproduced with this procedure [34]. The low intensity peaks in figure 3 between 6 and 10 eV will be undetectable, also because of the presence of the main edge at these energies. An important difference between K pre-edge and L edge structures is that the L edges are strongly influenced by the multiplet effects of the 2p core hole, i.e. the 2p 3d two-electron integrals, that redistribute the states and intensities significantly. The 1s core

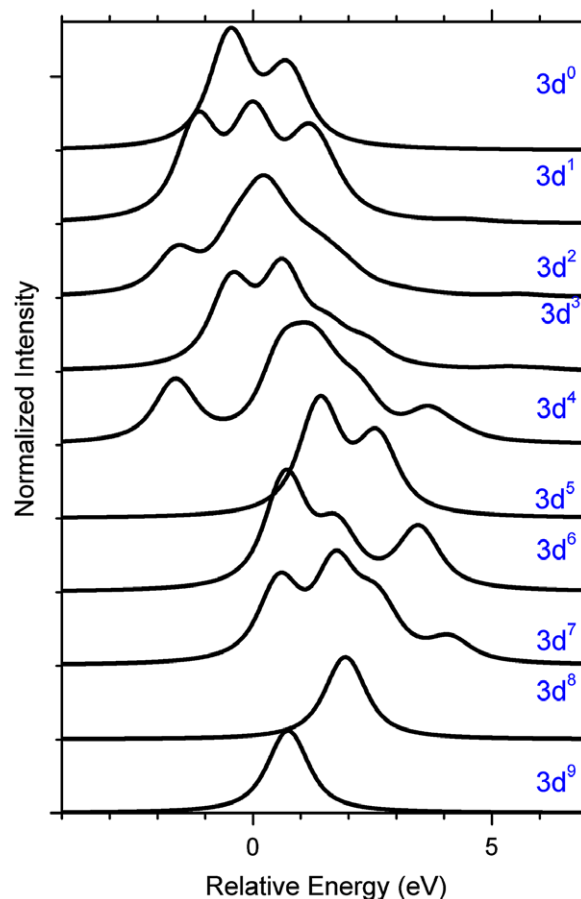


Figure 2. Crystal field multiplet calculations of the $3d^N$ to $1s^1 3d^{N+1}$ quadrupole transitions with a crystal field value $10 Dq$ of 1.2 eV. The zero energy is set to the average energy of the $3d^N$ initial states and the $1s^1 3d^{N+1}$ final states.

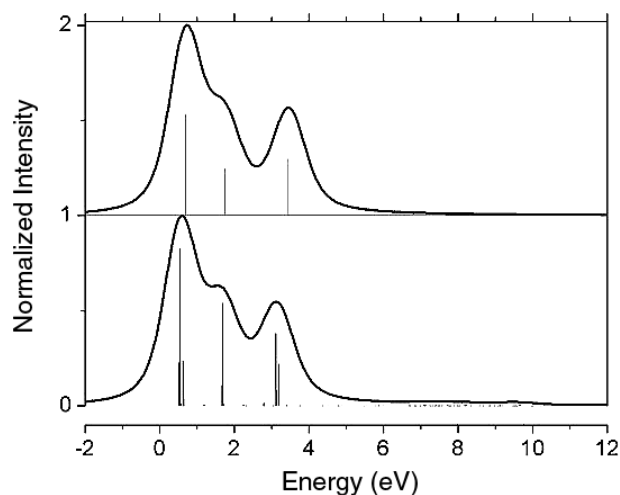


Figure 3. The comparison of a crystal field multiplet calculation (top) with a charge-transfer multiplet calculation (bottom) for a divalent iron coordination complex.

hole has essentially no effect (other than its charge) on the multiplet states, implying that they stay closer to their situation in the ground state.

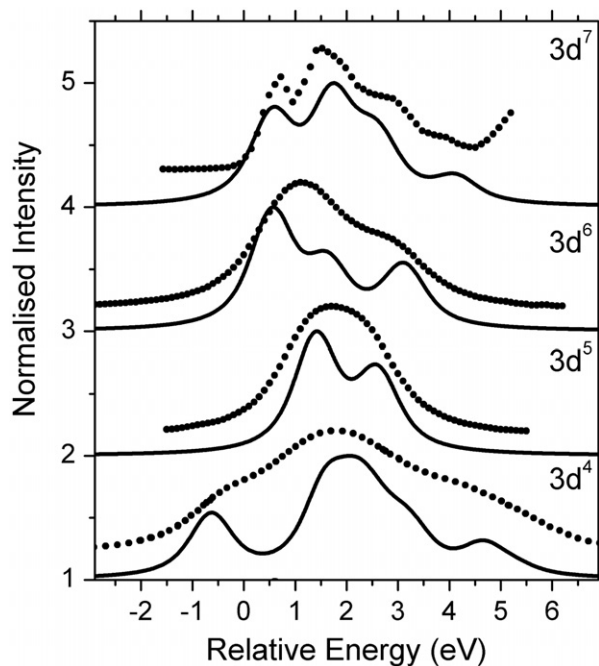


Figure 4. The pre-edge structures of the transition metal oxides Mn_2O_3 ($3d^4$), MnO ($3d^5$), Fe_2SiO_4 ($3d^6$) and CoO ($3d^7$) compared with the crystal field multiple calculations as reproduced from figure 2.

Tetrahedral transition metal coordination complexes, or in general systems where inversion symmetry is broken, have dipole–quadrupole mixing [31, 35]. In case of tetrahedral symmetry, the local dipole–quadrupole mixing *only* involves the t_2 -states, not e-states. This has been nicely shown for a series of titanium coordination complexes by de Beer *et al* [35]. Because inversion symmetry is broken, the metal 3d and 4p states mix with each other and form a set of combined 3d + 4p symmetry states. As such, the dipole (D) and quadrupole (Q) transitions reach the same final states, and their peaks are visible at the same energy.

3.2. The 1s XANES pre-edge structures in bulk oxides

The situation of bulk oxides is more complex, because in addition to the local effects, there can be effects due to translation symmetry and/or effects due to metal–metal charge transfer.

Figure 4 compares four experimental pre-edge structures with crystal field multiplet calculations. One can observe that the experimental spectral shapes are relatively well reproduced. The Mn_2O_3 ($3d^4$), MnO ($3d^5$) and Fe_2SiO_4 ($3d^6$) have been measured with HERFD-XANES with 1.0 eV overall resolution and CoO ($3d^7$) has been measured with 0.3 eV overall resolution. In all cases the constant emission energy (CEE) spectrum is given, in other words the partial fluorescence yield (PFY) spectrum at one particular emission energy. If high resolution is used the PFY spectrum can deviate from the actual x-ray absorption spectrum as will be discussed in section 3.3.

It is difficult to compare these results with the multiple scattering and band structure results as discussed above,

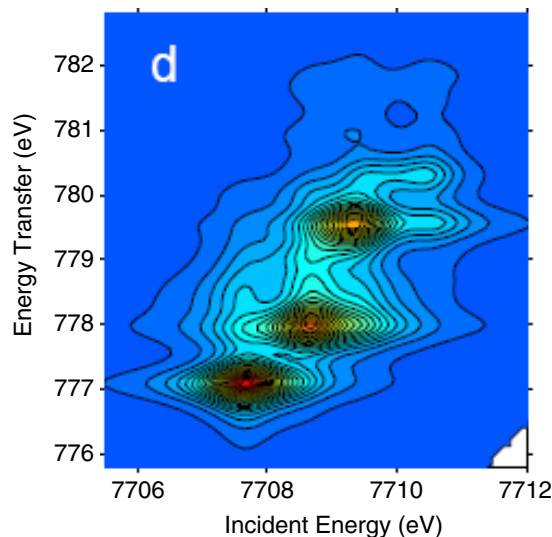


Figure 5. The matrix elements of the $3d^7 \rightarrow 1s^1 3d^8$ excitations and the $1s^1 3d^8 \rightarrow 2p^5 3d^8$ decay channels are calculated and inserted into the Kramers–Heisenberg formula.

because in most calculations that analyse the pre-edge structure of normal XANES spectra only a single peak is visible in both experiment and theory [8]. Exceptions are the DFT calculations of TiO_2 that reveal two dipole and two quadrupole peaks [16], but for this $3d^0$ system there is no difference between multiplet and DFT calculations. Recently, band structure calculations have been used to describe HERFD-XANES spectra. The Fe_2O_3 spectrum is reproduced by the density of states, as discussed in detail in section 3.4. Again, for this $3d^5$ system, there is no visible difference between multiplet calculations and the DFT results. Juhin *et al* analysed the angular dependence of the pre-edge structure of the Cr K edge of Cr^{3+} in MgAl_2O_4 . They show that the angular dependence can only be reproduced with crystal field multiplet calculations, while the DFT calculations do not correctly reproduce this effect [36].

We conclude that for all spectra where the pre-edge structure has been revealed, the crystal field multiplet calculations reproduce the observed spectra. In case of Cr^{3+} , Fe^{2+} and Co^{2+} ions in oxides these effects have not (correctly) been calculated by DFT based calculations.

3.2.1. The 1s 2p resonant x-ray emission spectrum of CoO.

The need for detailed (multiplet) calculations becomes more apparent from the 1s 2p resonant x-ray emission spectra, or alternatively the resonant inelastic x-ray scattering (RIXS). We will show the crystal field multiplet calculations for CoO as an example. The 1s 3d excitation is described as the transition from $3d^7$ to $1s^1 3d^8$ and the 1s 2p decay is described as the transition from $1s^1 3d^8$ to $2p^5 3d^8$.

Figure 5 shows the $3d^7 \rightarrow 1s^1 3d^8 \rightarrow 2p^5 3d^8$ transitions in CoO . The Kramers–Heisenberg formula is used and the matrix elements of the $3d^7 \rightarrow 1s^1 3d^8$ excitation and the $1s^1 3d^8 \rightarrow 2p^5 3d^8$ decay are included. The spectrum is broadened by the intermediate state 1s lifetime broadening, the final-state 2p lifetime broadening plus the

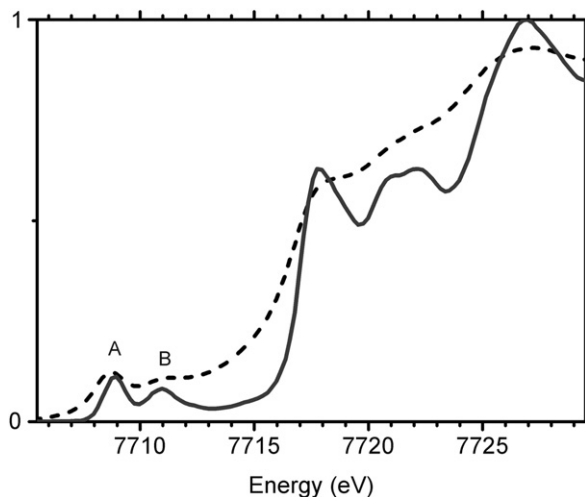


Figure 6. The cobalt 1s XANES spectrum of LiCoO_2 . Shown is the normal XAS spectrum (dashed), as measured with a solid state fluorescence detector and the HERFD-XANES spectrum (solid).

experimental resolution of the x-ray monochromator and the x-ray detector. The intermediate state 1s lifetime broadening plays a role in the denominator of the Kramers–Heisenberg formula and effectively determines the energy range in which states interfere. In case of CoO , the interference effects on the 1s 2p RIXS spectrum of CoO are significant due to the large overlap of the $1s^1 3d^8$ intermediate states [37]. An important result is that the 1s 2p RIXS spectrum contains many details that can be used for a more precise simulation and hence for a better description of the electronic structure. The recent high-resolution experiments agree with these calculations [37]. No additional structure is visible in experiment, other than these, coherent, $3d^7 \rightarrow 1s^1 3d^8 \rightarrow 2p^5 3d^8$ transitions. For the general interpretation of the pre-edge structures, this implies that the general model of the quadrupole pre-edge plus dipole edge is exactly confirmed in case of CoO .

3.3. The pre-edge structures in trivalent and tetravalent bulk oxides with inversion symmetry

Rutile TiO_2 , MnO_2 , LiCoO_2 and LaCoO_3 have crystal structures where both the metal–oxygen and the metal–metal bonds have inversion symmetry. We ignore the breaking of inversion symmetry by magnetic ordering for the moment. Inversion symmetry implies the absence of dipole–quadrupole mixing.

Figure 6 shows the cobalt K edge x-ray absorption spectra of LiCoO_2 . The normal K edge XANES spectrum is given in comparison with the HERFD-XANES. The peak at 7718 eV is related to the main edge, in other words to the dipole transitions to the 4p-band. The 1s XANES spectrum of LiCoO_2 contains two clearly observable pre-edges A and B. LiCoO_2 is a non-magnetic ($S = 0$) low-spin oxide and its ground state has a filled t_{2g} band and an empty e_g band. This implies the presence of a single 1s 3d quadrupole peak, which seems in contrast with the two peaks in experiment. Detailed angular dependent experiments showed that the first

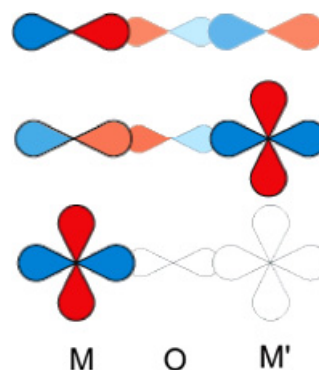


Figure 7. The final-state configurations of the 1s 4p dipole (top), the non-local 1s 4p(3d) dipole (middle) and the 1s 3d quadrupole (bottom) transitions.

peak (A) at 7709 eV has quadrupole nature and the second peak (B) at 7711 eV has dipole character [37]. This second pre-edge peak of dipole character is absent in a $\text{Co}(\text{aceto-acetate})_3$ coordination complex. Both systems are low-spin trivalent cobalt systems, where $\text{Co}(\text{acac})_3$ has isolated Co^{III} ions and LiCoO_2 contains oxygen mediated Co–Co interactions. These observations indicate that the first peak is the local 1s 3d quadrupole transition, while the second peak is a dipole 1s 4p transition to the 4p character of the 3d-band. Because of the inversion symmetry, this 4p character cannot mix with 3d character locally, but one can imagine the mixing of 4p character of a neighbouring Co atom into the 3d states of the Co atom, where the core hole is excited [37].

Figure 7 indicates the three types of final states, i.e. the 1s 4p dipole transition to the empty 4p-band (top), the 1s 4p dipole transition that is coupled to a 3d state of a neighbouring Co atom (middle) and the 1s 3d quadrupole transition into the local 3d states (bottom). Because the core hole is positioned at metal M, the bottom configuration feels a much stronger core-hole potential and as a result it is shifted to lower energy, compared with the middle situation, where the core-hole sites on M but the 3d state is localized at metal M'. These non-local pre-edge transitions have been observed for the low-spin trivalent cobalt oxides LiCoO_2 , AgCoO_2 , LaCoO_3 [37] and also for TiO_2 [16, 38, 39] and MnO_2 [40]. Shukla *et al* observed very small non-local transitions, alternatively called off-site transitions, in La_2CuO_4 [41].

3.4. The pre-edge structures in trivalent bulk oxides without inversion symmetry

Metal oxides without inversion symmetry allow the local mixing of 4p and 3d states. For example, Fe_2O_3 has the corundum structure where the Fe–Fe bonds are strongly deviating from inversion symmetry, with essentially aligned short and long Fe–Fe bonds. The pre-edge structure of Fe_2O_3 shows an angular dependent structure [42] that can be explained as a combination of dipole and quadrupole transitions. Figure 8 compares the pre-edge intensity ratio of the T_{2g} and E_g pre-edge peaks for dipole and quadrupole transitions. The intensity of the dipole transitions has been taken from Glatzel *et al* [42] and the quadrupole transitions

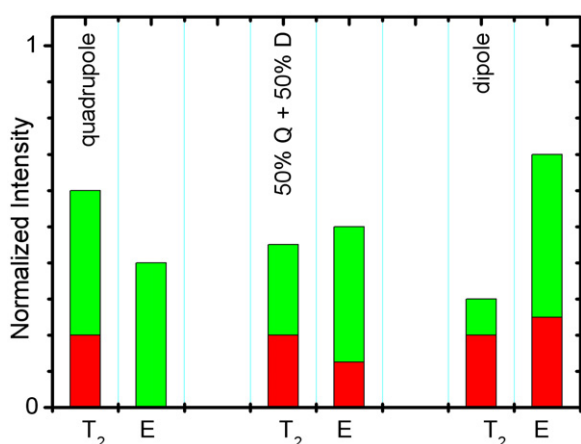


Figure 8. The quadrupole (left) and dipole (right) pre-edge intensities of respectively the T_{2g} and the E_g pre-peak in Fe_2O_3 . The angle-integrated intensities have been divided into intensity for an angle of 45° with the c -axis (red, bottom), respectively perpendicular to the c -axis (green, on-top). The middle bars are calculated assuming a 50:50 mixture of dipole and quadrupole transitions.

have been calculated as the $3d^6 \rightarrow 1s^1 3d^7$ multiplet transitions in C_{3v} symmetry. The quadrupole transitions have a larger T_{2g} pre-edge and the dipole transitions a larger E_g pre-edge. Both have an angular dependence where E_g pre-edge is favoured for the polarization perpendicular to the c -axis. The bars in the middle of figure 8 simulate a 50:50 mixture of dipole and quadrupole character, which reproduce the experimental results [42]. This indicates that the pre-edge structures of Fe_2O_3 have an approximately 50% dipole and a 50% quadrupole character. We note that this is at odds with the results by Dräger *et al* [43] and further experiments, e.g. angular dependent studies, are necessary. Because of the absence of the inversion symmetry, the 4p states and the 3d states can locally mix. The short Fe–Fe distance and large distortion from inversion symmetry explain the relatively large dipole component. Also the HERFD-XANES spectra of Fe_2O_3 indicate the presence of an additional pre-edge structure at higher energy, which would be consistent with it being a non-local transition similar to the oxides discussed in section 3.3. This interplay between local dipole transitions and non-local dipole transitions remains as yet an open issue that must be further studied [42].

4. Concluding remarks

We have given a consistent interpretation of the pre-edge structures in 1s XANES spectra of transition metal oxides and coordination complexes. Transition metal coordination complexes can be well described with a local model containing only one metal ion. Octahedral coordination complexes show weak pre-edge features due to the 1s 3d quadrupole transitions and tetrahedral coordination complexes have more intense pre-edge structures due to the local mixing of 3d and 4s states. The 1s 3d quadrupole transitions are calculated with the charge-transfer multiplet program for the $3d^N$ to $1s^1 3d^{N+1}$ multiplet transition.

Divalent transition metal oxides can be described similar to coordination complexes, but for trivalent, and tetravalent, oxides, additional structures are visible in the pre-edge region due to non-local dipole transitions, related to oxygen mediated metal–metal interactions. This yields additional intensity at the 3d-band region, which appears at a different energy than the local 1s 3d quadrupole transitions due to the smaller core-hole potential due to the delocalization of the excited electron.

The main edge of the 1s XANES can be accurately described with multiple scattering and band structure calculations. It turns out that in most cases, charge-transfer effects are not detectable and single electron excitation calculations find very good agreement.

Acknowledgments

Financial support for this research work from the Dutch National Science Foundation (NWO) in the form of a VICI grant (to FMFdG), the Hungarian Scientific Research Fund (OTKA) under contract No. K 72597 (to GV) and the Bolyai János Fellowship (to GV).

References

- [1] Rez P, Bruley J, Brohan P, Payne M and Garvie L A J 1995 *Ultramicroscopy* **59** 159
- [2] Cabaret D, Mauri F and Henderson G S 2007 *Phys. Rev. B* **75** 184205
- [3] Gaudry E, Cabaret D, Sainctavit P, Brouder C, Mauri F, Goulon J and Rogalev A 2005 *J. Phys.: Condens. Matter* **17** 5467
- [4] Schwarz K, Blaha P and Madsen G K H 2002 *Comput. Phys. Commun.* **147** 71
- [5] Milman V, Winkler B, White J A, Pickard C J, Payne M C, Akhmatkaya E V and Nobes R H 2000 *Int. J. Quantum Chem.* **77** 895
- [6] Joly Y 2003 *J. Synchrotron Radiat.* **10** 58
- [7] Rehr J J and Albers R C 2000 *Rev. Mod. Phys.* **72** 621
- [8] Wu Z Y, Xian D C, Hu T D, Xie Y N, Tao Y, Natoli C R, Paris E and Marcelli A 2004 *Phys. Rev. B* **70** 33104
- [9] Benfatto M, Della Longa S and Natoli C R 2003 *J. Synchrotron. Radiat.* **10** 51
- [10] Kutzler F W, Scott R A, Berg J M, Hodgson K O, Doniach S, Cramer S P and Chang C H 1981 *J. Am. Chem. Soc.* **103** 6083
- [11] Grunes L A 1983 *Phys. Rev. B* **27** 2111
- [12] Müller J E, Jepsen O and Wilkins J W 1982 *Solid State Commun.* **42** 365
- [13] Norman D, Garg K B and Durham P J 1985 *Solid State Commun.* **56** 895
- [14] Czyzyk M T, Potze R and Sawatzky G A 1992 *Phys. Rev. B* **46** 3729
- [15] Rehr J J and Ankudinov A L 2005 *Coord. Chem. Rev.* **249** 131
- [16] Cabaret D, Joly Y, Renevier H and Natoli C R 1999 *J. Synchrotron. Radiat.* **6** 258
- [17] Juhin A, Calas G, Cabaret D, Galois L and Hazemann J L 2007 *Phys. Rev. B* **76** 054105
- [18] Bair R A and Goddard W A III 1980 *Phys. Rev. B* **22** 2767
- [19] Tolentino H, Medarde M, Fontaine A, Baudelet F, Dartyge E, Guay D and Tourillon G 1992 *Phys. Rev. B* **45** 8091
- [20] Collart E, Shukla A, Rueff J P, Leininger P, Ishii H, Jarrige I, Cai Y Q, Cheong S W and Dhalenne G 2006 *Phys. Rev. Lett.* **96** 157004

- [21] Kau L S, Spira-Solomon D J, Penner-Hahn J E, Hodgson K O and Solomon E I 1987 *J. Am. Chem. Soc.* **109** 6433
- [22] Waychunas G A, Apter M J and Brown G E 1983 *Phys. Chem. Miner.* **10** 1
- [23] Wilke M, Farges F, Petit P E, Brown G E and Martin F 2001 *Am. Mineral.* **86** 714
- [24] Heijboer W M, Glatzel P, Sawant K R, Lobo R F, Bergmann U, Barrea R A, Koningsberger D C, Weckhuysen B M and de Groot F M F 2004 *J. Phys. Chem. B* **108** 10002
- [25] Radu D, Glatzel P, Gloter A, Stephan O, Weckhuysen B M and de Groot F M F 2008 *J. Phys. Chem. C* **112** 12409
- [26] Wong J, Lytle F W, Messmer R P and Maylotte D H 1984 *Phys. Rev. B* **30** 5596
- [27] Keller D E, de Groot F M F, Koningsberger D C and Weckhuysen B M 2005 *J. Phys. Chem. B* **109** 10223
- [28] Glatzel P and Bergmann U 2005 *Coord. Chem. Rev.* **249** 65
- [29] de Groot F and Kotani A 2008 *Core Level Spectroscopy of Solids* (New York: Taylor and Francis) p 3
- [30] Hämmäläinen K, Siddons D P, Hastings J B and Berman L E 1991 *Phys. Rev. Lett.* **67** 2850
- [31] Westre T E, Kennepohl P, DeWitt J G, Hedman B, Hodgson K O and Solomon E I 1997 *J. Am. Chem. Soc.* **119** 6297
- [32] Vankó G, Neisius T, Molnar G, Renz F, Karpati S, Shukla A and de Groot F M F 2006 *J. Phys. Chem. B* **110** 11647
- [33] Glatzel P, Bergmann U, Yano J, Visser H, Robblee J H, Gu W W, de Groot F M F, Christou G, Pecoraro V L, Cramer S P and Yachandra V K 2004 *J. Am. Chem. Soc.* **126** 9946
- [34] de Groot F M F, Glatzel P, Bergmann U, van Aken P A, Barrea R A, Klemme S, Hävecker M, Knop-Gericke A, Heijboer W M and Weckhuysen B M 2005 *J. Phys. Chem. B* **109** 20751
- [35] DeBeer-George S, Brant P and Solomon E I 2005 *J. Am. Chem. Soc.* **127** 667
- [36] Juhin A, Brouder C, Arrio M-A, Cabaret D, Saintavit P, Balan E, Bordage A, Seitsonen A P, Calas G, Eeckhout S G and Glatzel P 2008 *Phys. Rev. B* **78** 195103
- [37] Vankó G, de Groot F M F, Huotari S, Cava R J, Lorenz T and Reuther M 2008 arXiv:0802.2744
- [38] Shirley E L 2004 *J. Electron Spectrosc. Relat. Phenom.* **136** 77
- [39] Uozumi T, Okada K, Kotani A, Durmeyer O, Kappler J P, Beaurepaire E and Parlebas J C 1992 *Europhys. Lett.* **18** 85
- [40] Farges F 2005 *Phys. Rev. B* **71** 165109
- [41] Shukla A, Calandra M, Taguchi M, Kotani A, Vanko G and Cheong S W 2006 *Phys. Rev. Lett.* **96** 077006
- [42] Glatzel P, Mirone A, Eeckhout S G, Sikora M and Giuli G 2008 *Phys. Rev. B* **77** 115133
- [43] Dräger G, Frahm R, Materlik G and Brummer O 1988 *Phys. Status Solidi b* **146** 287